

Catalysis Science & Technology

Accepted Manuscript



This is an *Accepted Manuscript*, which has been through the Royal Society of Chemistry peer review process and has been accepted for publication.

Accepted Manuscripts are published online shortly after acceptance, before technical editing, formatting and proof reading. Using this free service, authors can make their results available to the community, in citable form, before we publish the edited article. We will replace this *Accepted Manuscript* with the edited and formatted *Advance Article* as soon as it is available.

You can find more information about *Accepted Manuscripts* in the [Information for Authors](#).

Please note that technical editing may introduce minor changes to the text and/or graphics, which may alter content. The journal's standard [Terms & Conditions](#) and the [Ethical guidelines](#) still apply. In no event shall the Royal Society of Chemistry be held responsible for any errors or omissions in this *Accepted Manuscript* or any consequences arising from the use of any information it contains.

COMMUNICATION

www.rsc.org/

Cite this: DOI: 10.1039/x0xx00000x
 Received 00th January 2012,
 Accepted 00th January 2012

Role of carbon atoms of supported iron carbides in Fischer-Tropsch synthesis

DOI: 10.1039/x0xx00000x

V.V. Ordonsky*, B. Legras, K. Cheng, S. Paul and A.Y. Khodakov*

High reactivity of iron carbides enhances Fischer-Tropsch reaction rate on supported iron catalysts. Highly dispersed carbide is easily hydrogenated to methane in the hydrogen atmosphere with subsequent regeneration in the presence of CO. Carbon atoms in iron carbide are involved in the initiation of chain growth in Fischer-Tropsch synthesis.

Fischer-Tropsch (FT) synthesis is an efficient way of valorization of syngas (H_2/CO mixtures) which can be produced from biomass, coal, natural or shale gases. FT synthesis is a complex surface polymerization reaction occurring on metal catalysts leading to methane and higher hydrocarbons. High temperature FT (HTFT) synthesis (300-350°C) is one of the most interesting routes for synthesis of alkenes and oxygenates. Both bulk and supported iron catalysts are used usually in high temperature FT synthesis. The catalyst activity in high temperature FT synthesis has been attributed to iron carbides (predominantly Fe_2C and Fe_3C_2). Iron carbides might form during pretreatment of iron catalyst in CO or syngas and they are stable under a wide range of reaction conditions. Both experimental and theoretical studies have been dedicated to the investigation of the mechanism of FT synthesis over Fe carbide catalyst.

Like any polymerization reaction, FT synthesis comprises several elementary steps: chain initiation, chain growth and chain termination. Both oxygenate and carbide mechanisms for FT polymerization have been discussed in the literature. The "carbide" mechanism has been initially proposed by Fischer and Tropsch [1] for bulk carbide and further for the hydrocarbon synthesis through surface carbide species. It involves full dissociation of CO into C and O with further hydrogenation of atoms [2-4]; hydrogen assisted dissociation of CO [5-6] and H interaction with non-dissociated CO [7]. On other hand, after the pioneering report by Emmett [8], the oxygenate mechanism of FT synthesis has seen a recent resurgence in works by Davis [9]. In the oxygenate mechanism, chain growth involves CO insertion which leads to hydrocarbons and oxygenates. Despite significant number of publications which have addressed chain growth in FT synthesis, much fewer information is available about chemical species involved in chain initiation.

Though several iron carbides are usually assumed to be the most active phases for FT synthesis in iron catalysts, very little

information is available about the role of carbon atoms in iron carbide in this reaction. Information about involvement of carbon atoms in iron carbides in different steps of FT synthesis can be obtained using isotope labeling. Kumer et al. [10] reported in the experiment with precarbidised Fe catalyst in ^{14}CO . The authors observed very small ^{14}C fraction (16 % at 300°C) in the reaction products and concluded that reduction of iron carbide was not a major reaction pathway in hydrocarbon formation. Bennett et al. [11, 12] studied the mechanism of methane and hydrocarbon formation over Fe/Al_2O_3 by labelling the feed mixture with ^{13}C and deuterium. The isotope labeling experiments showed that the exchange of ^{13}C carbon atoms in iron carbide with the reacting molecules was very slow. It was assumed that bulk iron carbide and deposited C on the surface did not participate in FT synthesis. A C-H species on the surface of the catalyst have been found to be responsible for hydrocarbon synthesis. Recently the hypothesis that iron carbide could be directly involved in FT synthesis has been supported by Niemantsverdriet et al [13] using DFT modeling of CO

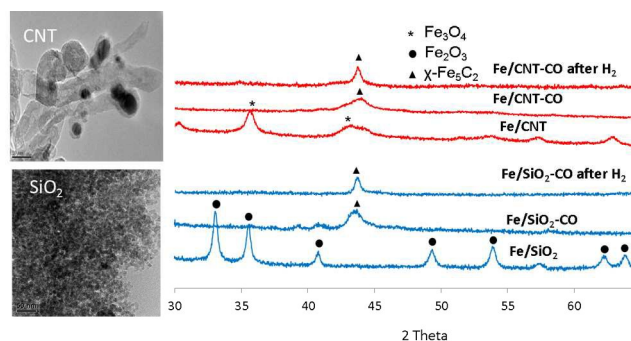


Figure 1. TEM and XRD analysis of Fe/CNT and Fe/SiO₂

hydrogenation over Fe_5C_2 . The proposed reaction cycle of CO hydrogenation to methane resembled the Mars-van Krevelen mechanism for partial oxidation and involved hydrogenation of iron carbides with release of 4-fold site for dissociation of CO molecule.

The present paper focuses on the elucidation of the role of carbon atoms of iron carbides in high temperature FT synthesis over iron catalysts supported by carbon nanotubes and silica using isotope labeling, steady state catalytic tests and catalyst characterization.

Table 1. Characterization and catalytic performance of Fe/CNT and Fe/SiO₂ (T=300°C, H₂/CO=2, GHSV=16200 cm³ g⁻¹ h⁻¹, P=20 bar)

Catalyst	Particle size, nm XRD analysis (TEM)			CH ₄ formation during hydrogenation CH ₄ /Fe		X _{CO} , %	Reaction rate, mmol/ g·h	S _{CO₂} , %	Product distribution, (% C _{at} , CO ₂ free)				C ₂ -C ₄ Olef/ Paraff
	After calcination	After CO treatment	After static hydrogenation	TPR	Static hydrogenation				CH ₄	C ₂ -C ₄ olef	C ₂ -C ₄ paraf	C ₅₊	
Fe/CNT	12(14)	4(13)	26.1	0.12	0.26	85	170	30	8.7	20.7	14.7	55.9	1.4
Fe/SiO ₂	17(14)	6(12)	20.4	0.04	0.25	28	56	13	12.8	20.6	12.5	54.1	1.6

Conventional Fe/CNT and Fe/SiO₂ catalysts (10 wt. % Fe) were prepared by incipient wetness impregnation of carbon nanotubes and silica with iron nitrate solutions followed by drying and calcination. Further details about catalyst synthesis and characterization are available in Supporting Information (SI). The BET surface areas of Fe/CNT and Fe/SiO₂ were 160 and 307 m²/g with average pore diameters of 5 and 17 nm respectively. Magnetite (Fe₃O₄) was the major iron phase in the calcined Fe/CNT catalyst with an average crystallite size of 12.3 nm measured from the Scherrer broadening, while mostly hematite (Fe₂O₃) crystallites of 17.5 nm were detected in the calcined Fe/SiO₂ counterpart. These results correlate with the sizes determined by TEM (Table 1, Figure S1)

XPS, magnetization and Mossbauer measurements conducted earlier for the Fe/SiO₂ and Fe/CNT catalysts [14] show that catalyst activation in carbon monoxide at 350°C results in the formation of iron carbide nanoparticles with diameters 6 and 4 nm, respectively (Table 1, Figure 1). The silica supported samples also showed the presence of iron silicate species which do not carbide during the pretreatment in carbon monoxide. In Fe/CNT, considerable concentrations of magnetite were still observed after the extended catalyst treatment in CO at 350°C [14]. This enhanced stability of magnetite in carbon nanotubes could be attributed to the strong interaction between magnetite and carbon support which could affect the catalytic performance. The iron nanoparticles encapsulated by carbon nanotubes was observed by TEM in Fe/CNT (Figure 1). TEM does not show any major decrease in iron particle size after carbidisation (Table 1, Figure S1). This observed discrepancy can be attributed to the fact that XRD measures only the size of iron carbide ordered crystalline domains, while TEM can detect both iron individual carbide crystallites and crystallite agglomerates.

Catalytic performance of supported iron catalysts. Table 1 shows the catalytic performance data for Fe/CNT and Fe/SiO₂ catalysts pretreated with CO at 350°C. The catalytic activity of Fe/CNT was significantly higher compared to Fe/SiO₂. The olefins to paraffin ratio over Fe/CNT is 1.4 in comparison with 1.6 over Fe/SiO₂. No visible catalysts deactivation was observed after several days of catalytic testing (Figure S2).

Different intrinsic catalytic performance of silica and carbon nanotube supported catalysts was attributed to the different type and concentration of active sites in the catalysts. The higher activity of Fe/CNT was explained earlier by Bao and coworkers [15] by a confinement effect of iron particles in the CNT channels. According to the authors, the confinement of iron inside of the CNT with

unique electronic properties significantly modifies the catalytic performance [16]. The high activity of small carbide “nodules” forming shell on the surface of the core magnetite phase was proposed as an efficient catalytic system on silica supported catalysts [17]. Our results suggest that magnetite itself is inactive in FT synthesis. However, the composite of magnetite–carbide with highly active defected carbide phase could be involved in FT reaction over Fe/CNT [13]. The concentration of carbide could be also smaller in silica sample due to the lower extent of carbidisation of Fe/SiO₂ by formation of silicate species. The calculated Mössbauer parameters show significant contribution of oxide in this catalyst (Figure S3).

Reactivity of iron carbide species. The reactivity of iron carbides present in Fe/CNT and Fe/SiO₂ pretreated in CO was studied in hydrogen flow at 300°C and 20 bar with periodic analysis of the reaction products by GC (Figure 2). Methane was the major product on both Fe/CNT and Fe/SiO₂. Production of other light C₂-C₄ hydrocarbons has been observed of the reaction on both catalysts at the beginning of static hydrogenation. The fact might be explained by the presence of hydrocarbon fragments with C-C bonds on the surface of carbide nanoparticles. These species might be similar to those C-H species which were previously observed by Stockwell [11] as being responsible for hydrocarbon synthesis.

Interestingly, the initial methanation rate was significantly higher on carbidized Fe/CNT in comparison with Fe/SiO₂ (Figure 2). The methane formation over the carbidized Fe/CNT rapidly decreases during the first hour. The initial rate of methane formation is 2 times lower on Fe/SiO₂; it remains stable during the first two hours of the reaction. Integration shows that the amount of methane produced at 300°C is only 2 times lower (Table 1) on both Fe/SiO₂ an Fe/CNT in comparison with the calculated amount assuming complete hydrogenation of iron carbides (0.4 for Fe₃C₂). The XRD analysis (Figure 1) shows narrowing of iron carbide peaks after the treatment of both carbidized Fe/SiO₂ and Fe/CNT in hydrogen. The crystallite size evaluation using the Scherrer equation suggests an increase in the average particle size in Fe/CNT from 4 to 26 nm and in Fe/SiO₂ from 6 to 20 nm (Table 1). The apparent increase in the average iron carbide crystallite size after hydrogen treatment can be attributed to selective hydrogenation of only very small iron carbide particles in hydrogen, while larger iron carbide crystallites seem to be not much affected by this pretreatment. This also suggests that large iron carbide nanoparticles do not participate in methane formation under these conditions.

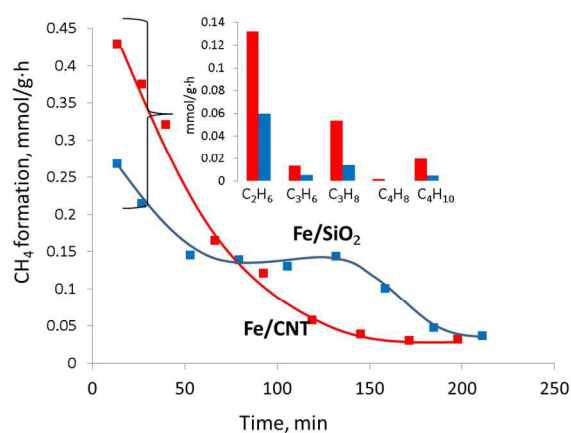


Figure 2. Methane formation rate in static hydrogenation of carbidised Fe/SiO₂ and Fe/CNT (Insert: rate of C₂-C₄ hydrocarbon production)

The catalysts after static hydrogenation can be again carbidised by pretreatment with CO or exposure to syngas under FT reaction conditions. Figure S4 shows the results of catalyst hydrogenation leading to methane production after carbidisation-hydrogenation cycle. The carbidisation was performed by catalyst exposure to CO at 350°C (4 h) and to syngas at 300°C (2 h). The results show almost identical kinetics of methane production after these cycles in both catalysts. This also suggests similar structure of active sites in the iron catalysts carbidised with CO and syngas.

The results of static hydrogenation conducted at hydrogen pressure of 20 bars are consistent with the TPR results (Figure S5). The TPR profile of Fe/CNT catalyst conducted at atmospheric pressure with 5% H₂/Ar flow shows the presence of low temperature peaks at 200 and 400°C which are not observed in the TPR profiles of the Fe/SiO₂ catalyst. This indicates higher reactivity of iron carbide species in the catalysts supported by carbon nanotubes. The higher carbide reactivity in CNT might be a result of disordered carbide structure located on the surface of magnetite in comparison with less reactive iron carbide over Fe/SiO₂. The in-situ XRD patterns measured in a 3% H₂/He flow at 400°C showed gradual decomposition of iron carbides into metallic iron on Fe/CNT catalyst (Figure S5). In the presence of relatively low partial pressure of hydrogen, iron carbides are completely decomposed into metallic iron at temperature higher than 400°C. Quantitative analysis (Table 1) indicates relatively small methane production in the TPR experiments. This suggests that exposure of iron carbides to higher temperature at relatively low hydrogen pressures principally lead to iron carbide decomposition (Fe₅C₂=5Fe+2C), while only small fractions of relatively reactive iron carbide are hydrogenated to methane. Thus, both static hydrogenation and TPR results indicate higher reactivity of iron carbides in Fe/CNT relative to Fe/SiO₂ which also coincides with higher FT reaction rate on Fe/CNT.

It should be mentioned that the initial rate of methane formation is significantly lower in comparison with time yield during FT synthesis at the similar conditions (Figure 1, Table 1). However, it should be taken into account that in the case of catalyst hydrogenation carbide cannot be regenerated like during FT

synthesis. It indicates on the high rate of regeneration of carbide from Fe in the case of participation of carbon of carbide in the FT synthesis.

Role of iron carbide in formation of higher hydrocarbons.

Carbon atoms in iron carbides can play multiple roles in FT synthesis. They may be hydrogenated to methane, initiate chain growth or can be directly converted into hydrocarbons. Isotope labeled carbon compounds are used in this work to identify the role of iron carbides in synthesis of long-chain hydrocarbon. The ¹³C labeled iron carbide was obtained by carbidisation of the calcined Fe/CNT using ¹³CO.

The first set of experiments addressed hydrogenation of labeled iron carbides. The hydrogenation led to mostly ¹³CH₄ methane production. The contribution of ¹²C in the formation of methane was negligible in comparison with ¹³C (Figure S6). This suggests that methane is produced from iron carbide species which form on the catalyst surface during carbidisation with ¹³CO. Note that carbon species of carbon nanotubes consisting of ¹²C seem not to be involved in the methane formation. The catalyst has been hydrogenated after the test and has shown very significant consumption of labeled carbide after reaction (Figure S6).

The objective of the second set of experiments was to identify

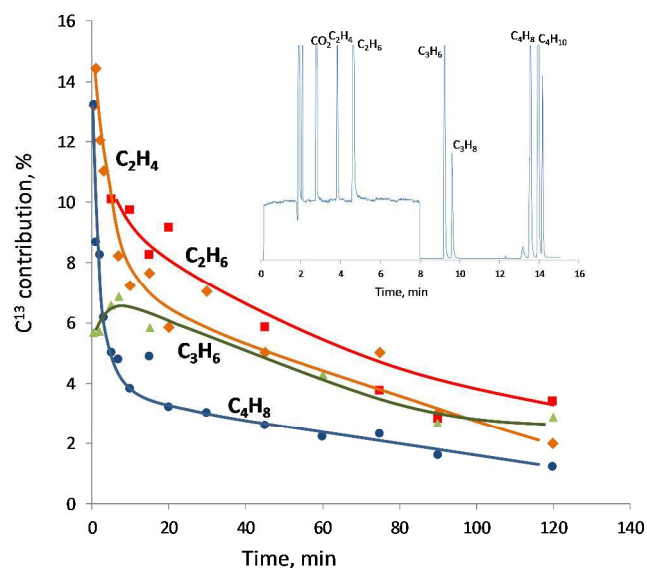


Figure 3. ¹³C fraction in the reaction products of FT synthesis over ¹³C labelled iron carbide supported by CNT (Insert: typical GC-MS pattern)

the role of labeled iron carbide in the production of higher hydrocarbons in FT synthesis. The ¹³C iron carbide species in carbidised Fe/CNT catalysts were exposed to the flow of ¹³CO and H₂ at 300°C. During the first 2 h of the test the isotope composition of the reaction products was periodically analyzed by GC-MS.

Several ¹³C labeled reaction products were detected which indicate participation of carbide species in FT reaction. The initial fraction of ¹³C in C₂-C₄ hydrocarbons was between 10 and 16 % (Figure 3). The contribution of ¹³C decreases however with time for all hydrocarbons which is due to consumption of labeled carbon from carbide. Careful analysis isotope distribution by combination of

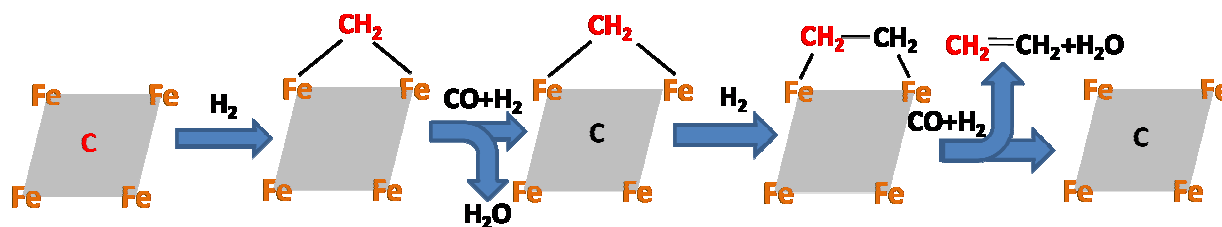


Figure 4. Chain growth pathways in FT synthesis on supported iron catalysts

individual patterns (SI) indicated the presence of only one ^{13}C atom in the forming $\text{C}_2\text{-C}_4$ olefins and paraffins in FT results. Note that the amount of multiple labeling was negligibly small. This suggests that labeled carbon of carbide does not form hydrocarbons itself but can initiate the chain growth. Afterwards, the active site might be regenerated by CO with formation of carbide and continuation of the growing chain. The contribution of labeled carbon decreases from ethylene to butylene (Figure 3) which is consistent with the assumption about participation of labeled carbon only in chain growth initiation. The chain reaction pathways are shown in Figure 4. The proposed growth schema also is in line with the Mars-van Krevelen mechanism for FT synthesis which was suggested earlier [13] on the basis of DFT modeling. Stockwell [11] also indicated that several of the carbon atoms in a product molecule could have come from the same site. This corresponds to our conclusion about working active carbide center initiating and producing the whole hydrocarbon chain. The other possible explanation about participation of labelled carbon in the formation of hydrocarbons could be in the fast CO dissociation with carbon-carbon exchange in the carbide species and formation of labelled ^{13}CO . However, in this case ^{13}C contribution would be the same for all hydrocarbons with their multiple labelling.

Note that the initial fraction of ^{13}C is somewhat smaller than that, assuming that the chain growth initiated selectively by ^{13}C -labelled iron carbide. This could be due to the hydrodynamic inertia of the reactor operating at high pressure, which leads to significant broadening of the transient responses. The other reason might be fast regeneration of carbide with ^{12}CO arriving from the gaseous phase and consecutive chain growth initiation on the forming ^{12}C iron carbides.

In summary, a combination of catalyst characterization, catalytic tests and isotope transient experiments suggests that initiation of chain growth in iron supported catalysts involves carbons atoms of iron carbides. The high activity of iron catalysts supported on carbon nanotubes relatively to the silica supported counterparts can be due to the higher reactivity and easy regeneration of supported iron carbide. Thus, it should result in the fast cycle of carbon incorporation in the growing chain.

Notes and references

Unité de Catalyse et de Chimie du Solide
UMR 8181 CNRS, Université Lille 1
Bât. C3, 59655 Villeneuve d'Ascq, France
Fax: (+33) 320 43 65 61
E-mail: vitaly.ordomsky@univ-lille1.fr

The authors gratefully acknowledge financial support for this work from the French National Agency for Research (Biosynop Project, Ref. ANR-11-BS07-026). The REALCAT platform is benefiting from a Governmental subvention administrated by the French National Research Agency (ANR) within the frame of the 'Future Investments' program (PIA), with the contractual reference 'ANR-11-EQPX-0037'. K. C. thanks the China Scholarship Council (CSC 201206310049) for a fellowship to support his one-year stay at the UCCS.

† Electronic Supplementary Information (ESI) available: [Preparation of catalysts; Characterization; Catalytic tests; Catalytic activity; Hydrogenation of carbides]. See DOI: 10.1039/c000000x/

- 1 F. Fischer, H. Tropsch, *Brennst. Chem.*, 1926, **7**, 97.
- 2 A.T. Bell, *Catal. Rev. Sci. Eng.*, 1981, **23**, 203.
- 3 A. Erdohelyi, F. Solymosi, *J. Catal.*, 1983, **84**, 446.
- 4 S.A. Eliason, C.H. Bartholomew, *Appl. Catal. A: Gen.*, 1999, **186**, 229.
- 5 O.R. Inderwildi, S.J. Jenkins, D.A. King, *J. Phys. Chem. C* 2008, **112**, 1305.
- 6 M. Ojeda, R. Nabar, A.U. Nilekar, A. Ishikawa, M. Mavrikakis, E. Iglesia, *J. Catal.* 2010, **272**, 287.
- 7 W.K. Hall, R.J. Kokes, P.H. Emmett, *J. Am. Chem. Soc.* 1960, **82**, 1027.
- 8 H.H. Podgurski, J.T. Kummer, T.W. DeWitt, P.H. Emmett, *J. Am. Chem. Soc.* 1950, **72**, 5382
- 9 B.H. Davis, *Catal.Today* 2009, **141**, 25.
- 10 J.T. Kummer, T.W. Dewitt, P.H. Emmett, *J. Amer. Chem. Soc.* 1948, **70**, 3632.
- 11 D.M. Stockwell, D. Bianchi, C.O. Bennet, *J. Catal.* 1988, **113**, 13.
- 12 H. Matsumoto, C.O. Bennet, *J. Catal.* 1978, **53**, 331.
- 13 J.M. Gracia, F.F. Prinsloo, J.W. Niemantsverdriet, *Catal. Lett.* 2009, **133**, 257.
- 14 K. Cheng, V. Ordonsky, M. Virginie, B. Legras, P. Chernavskii, V. Kazak, C. Cordier, S. Paul, Y. Wang, A. Khodakov, *Appl. Catal. A* 2014, **488**, 66.
- 15 W. Chen, Z.L. Fan, X.L. Pan, X.H. Bao, *J. Am. Chem. Soc.* 2008, **130**, 9414.
- 16 R.C. Haddon, *Science* 1993, **261**, 1545.
- 17 J. Xu, C.H. Bartholomew, *J. Phys. Chem. B* 2005, **109**, 2392.